Journal of Crystal Growth **20** (1973) 283–291 © *North-Holland Publishing Co.*

MELT COMPOSITIONS OF II–VI COMPOUNDS DURING CRYSTAL GROWTH IN A HIGH-PRESSURE FURNACE

HIROSHI KIMURA and HIROYOSHI KOMIYA

Central Research Laboratories, Mitsubishi Electric Corporation, Minamishimizu, Amagasaki-shi, Japan

Received 30 July 1971; revised manuscript received 23 August 1973

The melt compositions of ZnS, CdS, ZnSe, ZnTe, CdSe, and CdTe during crystal growth in a high-pressure Bridgman furnace have been investigated by the chemical analysis of quenched melts. The following results are obtained: (1) the melt compositions are essentially stoichiometric for ZnS, Cd-rich for CdS, and chalcogen-rich for the selenides and tellurides, and (2) the melt compositions are very close to stoichiometric for the sulfides and selenides, but for the tellurides they deviate considerably from the stoichiometric composition. These results have been analyzed on the basis of a simple model which assumes that the component gases of the compound diffuse out of the crucible containing the melt slowly enough for three-phase equilibrium to be maintained inside the crucible. According to this model the observed melt composition depends on the relative diffusion rates of the metal and chalcogen gases and on the relationship between the partial pressures of these gases and the melt composition.

1. Introduction

The technique of melt growth under a high pressure of an inert gas has been developed[1]) for growing crystals of volatile materials. This technique is mostly applied to II–VI compounds, which have high melting temperatures and not insignificant vapor pressures. Of these compounds, only CdTe (m.p. 1092 °C) can be grown by using a conventional Bridgman technique in which the melt is sealed in a quartz ampoule. In extending this technique even to ZnTe and CdSe, the danger of explosion is always present, because their melting points (1290 and 1255 °C, respectively) exceed the softening point of quartz.

In the high-pressure technique, crystals are grown from the melt by a Bridgman method under an inert gas pressure of the order of 100 atm. This pressure reduces the diffusion of the compound vapor from near the surface of the melt, thus decreasing the evaporation rate of the compound. The vapor over a II–VI compound is dissociated almost completely into atoms of the Group II element and molecules of the Group VI element. Because of the difference between the diffusion rates of these species, the composition of the melt does not in general remain stoichiometric during growth. Since the melt composition significantly influences the growth process and the characteristics of as-grown crystals, it is important to know how this composition changes during growth.

In this study, the melt compositions of six II–VI compounds in a high-pressure furnace have been investigated under various conditions by using wet chemical and electron microprobe techniques to analyze quenched boules. A semiquantitative analysis on the basis of a simple model accounts quite well for the experimental results and gives a general explanation of the variation in melt composition during crystal growth in a high-pressure furnace.

2. Experimental procedure

For ZnS, ZnSe, CdS and CdSe, the starting materials are commercially available powders of 99.999 % purity. ZnTe and CdTe are synthesized from the elements of 99.999 % purity in evacuated quartz ampoules at 900 °C and then crushed. The powders are preheated in a stream of either Ar or H_2 gas for one hour at 800 °C to 1300 °C, depending on the compound.

The high-pressure furnace having a graphite heater is similar to the one described in the review by Fischer[2]), but the graphite crucible containing the melt is moved from outside the furnace by a magnetic coupling mechanism. Fig. 1 shows a cross section of a typical crucible (a), with an example of the temperature profile inside the furnace (b). The profile changes somewhat depending on the temperature and on the inert gas pressure, but this change is not large enough to have a significant effect on the results of the present study.

In each run, 30 to 40 g of compound power is placed

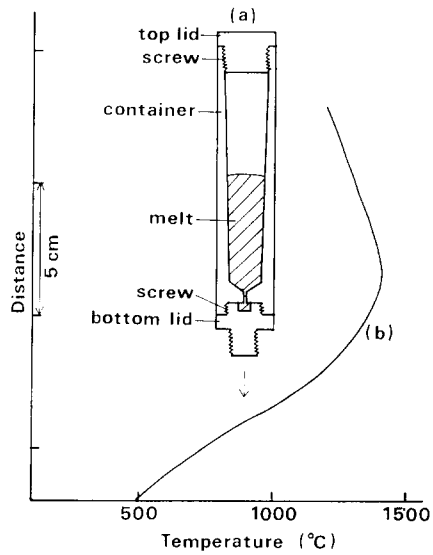

Fig. 1. (a) Graphite crucible used in high pressure crystal growth, and (b) typical temperature profile in the high-pressure furnace.

in a crucible. Before raising the temperature, the furnace is evacuated and then flushed with Ar gas, and this procedure is repeated several times. The furnace is then heated to 800 °C under vacuum and is kept evacuated at 800 °C for half an hour to bake out. After baking out, the exhaust valve is closed and the heating power is turned off. The furnace is then filled with Ar gas to about 100 atm and heated to the operating temperature within 15 to 20 min from about 300 °C. The maximum temperature is kept about 100 °C higher than the melting point of the compound. After an equilibration time of about half an hour, the crucible is lowered at the rate of 3 to 15 mm/h to start crystallization of the melt. When the crucible reaches a suitable position, the remaining melt is quenched by turning off the power and lowering the crucible at a velocity of about 35 mm/min. The temperature gradient in the vicinity of the melting point is about 60 °C/cm. It is difficult to estimate the cooling rate in the melt, but the temperature inside the furnace decreases by 200 °C within 45 sec and by 300 °C within 80 sec after the power is turned off.

The quenched boule has, in general, the features shown schematically in fig. 2. In the case of transparent compounds, region (2) looks as transparent as region (1), which was crystallized before quenching, except that a considerable number of small precipitates are found in region (2) by microscopic observation. The good crystalline quality of region (2) might have resulted because the cooling rate during quenching was not very fast, due to the heat capacity of the system. Region (3) is opaque and very fine-grained. For melts that were not stoichiometric, the electron microprobe trace shows that the precipitates of the excess element are much more highly concentrated in region (3) than in region (2). Apparently most of the excess element is rejected from region (2) during its crystallization and diffuses into region (3). In order to avoid errors due to this inhomogeneity, a disk about 1 mm thick was cut from the middle part of the quenched boule, as shown in fig. 2(a), to obtain samples for chemical analysis. The whole disk was crushed in a mortar to about 400 mesh, and the crushed powder was homogenized by mixing. The homogenized powder should have the same composition as the melt because, in the middle part of the quenched region, the rejection of the excess element from the upper and lower ends can be neglected and the excess element moves only in a horizontal direction. This was confirmed by the fact that several disks cut at different vertical positions in the middle part gave the same composition within the error of chemical analysis.

The amount of Zn or Cd in the homogenized powders was determined by using the standard EDTA titration technique with 0.01 molar EDTA solution and employing EBT solution as an indicator. The amount of Group VI element was determined by difference. Several samples were taken from each powder. Several others were taken from a crushed crystal of the same compound, and all samples were analyzed at the same time. It is believed that undoped crystals of II–VI compounds are nearly stoichiometric, that is, that the atom

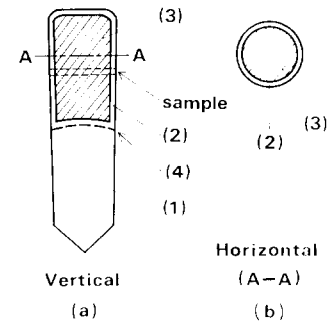

Fig. 2. Cross sections of a quenched boule. (1) Region crystallized before quenching. (2) Large-grain region crystallized during quenching. (3) Quenched region. (4) Solid-liquid interface just before quenching.

fraction of the Group II element differs from one-half by less than 10^{-3}. The measured atom fraction of the Group II element in the crystal samples (x in II_xVI_{1-x}) was therefore normalized to 0.500, and the normalization factor was used to correct the measured values for the amount of this element in the quenched samples. By this procedure, systematic errors in the EDTA analysis are corrected, and the value x in the quenched samples can be determined to an accuracy of $\Delta x = \pm 0.002$.

3. Experimental results

The preheated starting powder of each compound was also analyzed by EDTA titration. Typical results are listed in table 1. The starting powders of ZnSe and CdTe contain a little excess metal, but the other compounds are stoichiometric within the experimental error.

TABLE 1

Typical compositions of starting powders

Compound	Atom fraction of Group II_b element x
ZnS	0.501
CdS	0.502
ZnSe	0.512
CdSe	0.499
ZnTe	0.502
CdTe	0.515

Two to five quenched samples (boules) of each compound were investigated for a variety of experimental conditions. Table 2 gives one or more examples of the melt compositions measured for each compound by chemical analysis. In this table, x_f is the final melt composition, A_i and A_f are respectively the initial and final quantities of melt, t_g is the growth time, and v the growth rate of the crystal. C and μ_N/μ_M are a proportionality constant and a material parameter, respectively, used in the calculation described in section 5.

The experimental results obtained by chemical analysis are summarized as follows:

(1) The melt is always stoichiometric within experimental error for ZnS, metal-rich ($x > 0.5$) for CdS, and chalcogen-rich ($x < 0.5$) for the selenides and tellurides.

(2) The deviation of the final melt composition from the stoichiometric composition is always small for the sulfides and selenides. For samples of one of these compounds the deviation depends only slightly on the growth conditions (two samples of ZnSe are listed in table 2 to illustrate this). In case of the tellurides, on the other hand, the final deviation is comparatively large and depends strongly on the growth conditions (three samples of ZnTe are listed as an illustration).

Observations on the quenched samples were also made with an electron microprobe analyzer. The results are shown in fig. 3, which includes photographs for each compound obtained with the characteristic X-rays of (a) the Group II element and (b) the Group VI element. In these photographs brighter regions are enriched in the element whose characteristic X-rays were used, and darker regions contain lower concentrations of that element. In order to obtain intensity standards, microprobe photographs were also taken for a melt-grown single crystal of each compound. The photographs in fig. 3 show that the ZnS sample contains only one phase, while each of the other samples consists of two phases. By comparison with the single crystal photographs, the major phase in each sample is found to be stoichiometric within the accuracy of the microprobe. The second phase is Cd-rich in CdS, Se-

TABLE 2

Experimental results and parameters used in calculations on quenching of II–VI melts

Compound	Sample	x_f	A_f (mole)	A_i (mole)	t_g (h)	v (mole/h)	C (mole/h atm $°K^{1/2}$)	μ_N/μ_M
ZnS	#1	0.499	0.185	0.513	4.5	0.025		
CdS	#1	0.504	0.254	0.415	6.3	0.007	0.00068	4.0
ZnSe	#1	0.487	0.065	0.338	7.3	0.016		
	#2	0.488	0.085	0.381	9.0	0.014		
CdSe	#1	0.497	0.035	0.418	5.3	0.034	0.0020	0.59
ZnTe	#1	0.408	0.152	0.425	6.5	0.018	0.0025	
	#2	0.390	0.073	0.301	6.7	0.014	0.0019	0.091
	#3	0.359	0.074	0.301	7.0	0.014	0.0023	
CdTe	#1	0.414	0.056	0.208	5.5	0.010	0.013	0.25

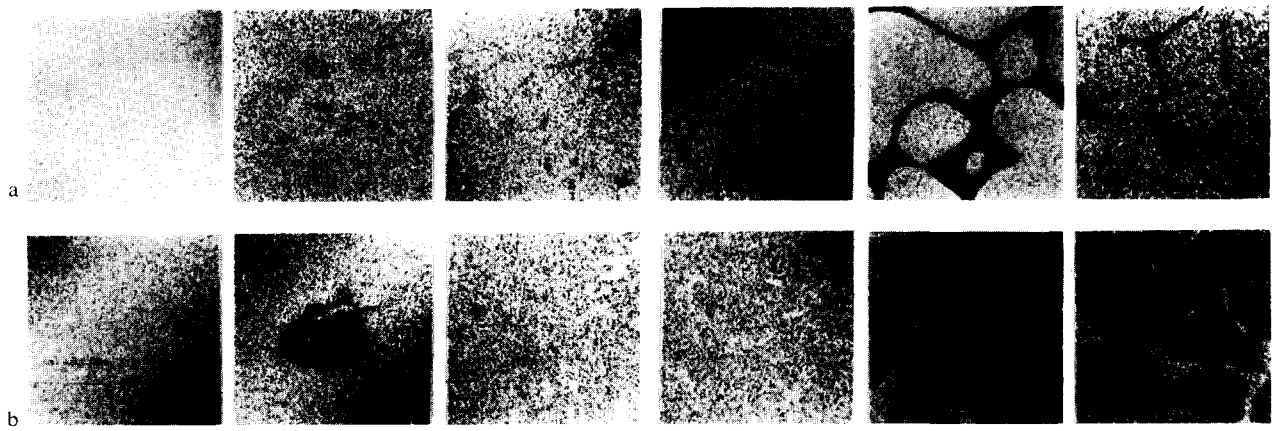

Fig. 3. Electron microprobe photographs (× 170) of quenched samples obtained by using characteristic X-rays of (a) Group II and (b) Group VI elements.

rich in ZnSe and CdSe, and Te-rich in ZnTe and CdTe. In each case the excess element identified by microprobe analysis is the same as the one found by chemical analysis. However, the fraction of the excess element in the second phase was not determined, because it is not easy to measure this quantitatively by microprobe analysis.

4. Effect of melt composition on crystal growth and electrical properties

The characteristic behaviour of the melt composition of each compound during crystal growth in a high-pressure furnace will influence the growth processes and also the electrical properties of as-grown crystals. In the growth of telluride crystals, the melt composition becomes increasingly Te-rich with increasing growth time, and a large amount of excess Te must be rejected at the interface between the growing crystal and the melt. Therefore the growth rate for tellurides cannot exceed the rate at which the excess Te can be rejected without causing constitutional supercooling. We observe that when the growth velocity exceeds 5 mm/h the crystal boule becomes very polycrystalline and a large single crystal cannot be obtained. It also appears that the final stage of growth may be taking place from Te-rich solutions, since dendrites are frequently found at the top of the crystals.

For selenide melts, the deviations from the stoichiometric composition are small compared with those of telluride melts. Nevertheless, the rejection of the excess Se from the growing crystals might still be one of the factors which limit the growth rate. When the growth velocity exceeds 8 mm/h, highly polycrystalline boules are obtained instead of single crystals. Melts of the sulfides are nearly stoichiometric, so that the necessity of rejecting the excess element at the interface should be less influential in limiting the growth rate. This might account for the success of Kozielski[3]) in growing ZnS crystals in a high-pressure furnace at the velocity of about 60 mm/h.

The melt compositions during the crystal growth of II–VI compounds in a high-pressure furnace also affect the electrical properties of the as-grown crystals, because these properties are determined by the crystals' deviations from stoichiometry as well as by their impurity content. The native defects associated with excess metal (chalcogen vacancies or metal interstitials) are donors, while those associated with excess chalcogen (metal vacancies or chalcogen interstitials) are acceptors. With rare exceptions, the compounds other than CdTe exhibit only one conductivity type, so that changes in composition and therefore in defect concentration change the resistivity but not the type. Thus donor-doped or nominally undoped ZnS, ZnSe, CdS, and CdSe are always n-type; the resistivity is relatively low for metal-saturated samples but extremely high for chalcogen-saturated ones. (In a few cases p-type conductivity has been reported in acceptor-doped ZnSe samples.) For ZnTe the situation is reversed: undoped or acceptor-doped crystals are always p-type, with higher resistivities for Zn-saturated samples than for Te-saturated ones. For CdTe, nominally undoped

samples are generally n-type if Cd-saturated and p-type if Te-saturated.

In view of these characteristics of the II–VI compounds, the electrical properties of crystals grown in a high-pressure furnace are in most cases consistent with the melt compositions determined by chemical analysis. As-grown crystals of CdS, both undoped and donor-doped, are n-type with low resistivities of the order of 10 ohm cm or below, while high-resistance crystals are easily obtained by heat treatment in S vapor after growth. On the other hand, both donor-doped and undoped ZnSe crystals are n-type but usually have high resistivities above 10^5 ohm cm, which can easily be decreased by heat treatment in Zn vapor. These properties are reasonably expected from the melt compositions, since CdS melts are Cd-rich, while ZnSe melts are Se-rich. As-grown crystals of undoped ZnTe and CdTe are p-type and usually have low resistivities of the order of 10 ohm cm or below, as expected because the melt compositions of ZnTe and CdTe are always Te-rich. As-grown crystals of ZnS are n-type with resistivities exceeding 10^8 ohm cm. Since heat treatment in Zn vapor is not as effective for ZnS as for ZnSe, it is not clear whether or not the high resistivity arises from the essentially stoichiometric melt composition of ZnS. In the case of CdSe, as-grown crystals are n-type with low resistivities of the order of 10 ohm cm. However, this is unexpected because the melt composition is Se-rich, and some other factors may be dominant.

5. Analysis

To interpret the experimental results on melt composition, an analysis was attempted on the basis of two fundamental assumptions. The first assumption is that the crystal is grown from the melt in a crucible which is not gas-tight, so that the component gases of the compound slowly diffuse out into the inert gas space through the crucible wall or through small gaps between the container and the lids. The leakage rate Y_i of each component gas is proportional to its concentration n_i (the number of atoms or molecules per unit volume in the crucible) and to its diffusion coefficient D_i,

$$Y_i \propto D_i n_i \propto D_i p_i / T, \tag{1}$$

where p_i is the partial pressure of the component gas and T is the absolute temperature. The derivation of eq. (1) will be given in the appendix.

The second basic assumption is that the solid, liquid, and gas phases within the crucible are in equilibrium among themselves at the liquidus temperature T. The partial pressures of the component gases p_M and p_N are therefore determined by T and by the composition of the liquid x. (The suffixes M and N indicate the Group II and Group VI element, respectively.) We can now write the rate of change of the total numbers of moles of metal [M] and of chalcogen [N] which are present in the liquid and vapor phases in the crucible,

$$\mathrm{d[M]}/\mathrm{d}t = C_1 (D_M p_M / T) - v, \tag{2a}$$

$$\mathrm{d[N]}/\mathrm{d}t = C_1 (2 D_N p_N / T) - v, \tag{2b}$$

where v is the crystal growth rate in moles per unit time, and C_1 is a proportionality constant. The vapor species are assumed to be metal atoms and diatomic chalcogen molecules. (The factor 2 in eq. (2b) results because the chalcogen molecule is diatomic.)

Because the amount of either component in the vapor phase is very small compared to the amount in the liquid phase, [M] and [N] in eq. (2) are approximately equal to the values in the liquid:

$$[\mathrm{M}] = Ax, \qquad [\mathrm{N}] = A(1-x), \tag{3}$$

where A is defined as the total number of moles of both components in the liquid. Unfortunately, we have neither experimental data nor theoretical expressions for D_i in the present system. However, according to the classical expression,

$$D_i = C_2 (T^{3/2}/P_0) \mu_i, \tag{4}$$

where C_2 is another proportionality constant and p_0 is the pressure of the inert gas, which is usually two orders of magnitude higher than those of the component gases. The material parameter μ_i is a property of the gas atom or molecule but independent of the experimental conditions.

If we substitute eq. (3) for [M] and [N] and (4) for D_i in eq. (2), we obtain rate equations for A and x:

$$\mathrm{d}A/\mathrm{d}t = -CT^{1/2} \{p_M + 2(\mu_N/\mu_M) p_N\} - 2v, \tag{5a}$$

$$\mathrm{d}x/\mathrm{d}t = A^{-1} [CT^{1/2} \{(x-1) p_M + 2x (\mu_N/\mu_M) p_N\} + (2x-1) v], \tag{5b}$$

where $C = C_1 C_2 \mu_M / p_0$.

To integrate eq. (5) numerically, we need analytical expressions for T, p_M and p_N as functions of x. The expressions given by Jordan[4]) were used for this purpose.

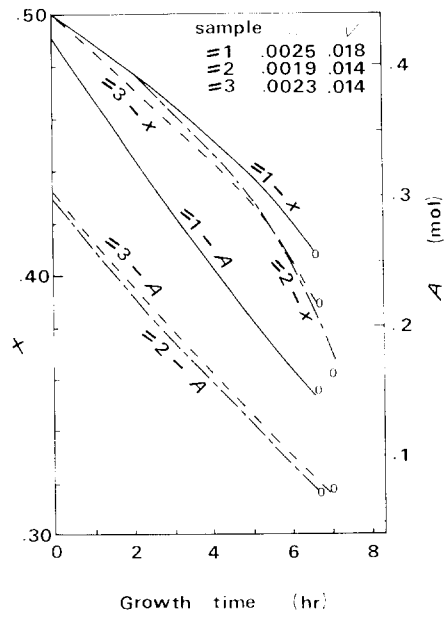

Fig. 4. Calculated $A(t)$ and $x(t)$ curves for three ZnTe samples.

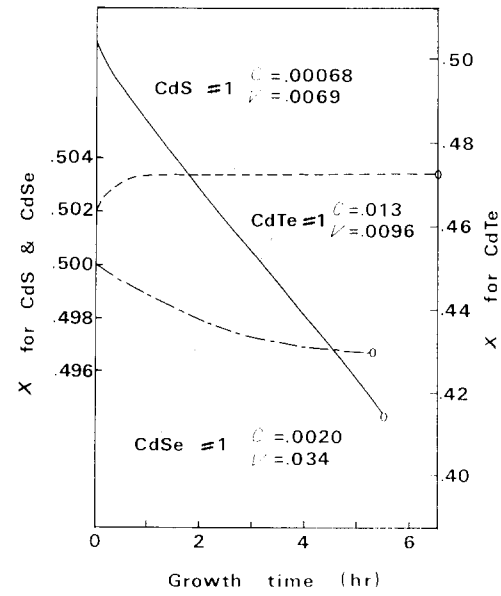

Fig. 5. Time variation of melt composition x for CdS, CdSe, and CdTe.

The values of the parameters to be used in these expressions were determined by using the experimental x–T and p–T relations obtained for ZnTe by Kulwicki[5]) and Shiozawa et al.[6]), for CdTe by Lorentz[7]) and Jordan and Zupp[8]), for CdSe by Reisman et al.[9]) and Burmeister and Stevenson[10]), and for CdS by Woodbury[11]) and Shiozawa and Jost[12]). These relations have not been determined for ZnS or ZnSe. In the calculations of $A(t)$ and $x(t)$, the measured quantities characterizing the experimental conditions are the composition x_i and total amount A_i of the starting powder, the growth time t_g, and v, which for simplicity is assumed to be constant with time. The values obtained as experimental results for the quenched melt are x_f and A_f. Both C and (μ_N/μ_M) are treated as adjustable parameters whose values are selected to make the calculated values of x_f and A_f agree with the experimental ones. The ratio (μ_N/μ_M) must be the same for all samples of a given compound. The value of C is expected to change somewhat from run to run because it depends on how tightly the crucible lid is fastened, even if the same crucible and inert gas pressure are used.

The calculations were performed for all samples except those of ZnS and ZnSe. The values of C and (μ_N/μ_M) used are listed in table 2. Fig. 4 shows the calculated time dependence of A and x for several samples of ZnTe, where the circles indicate the experimentally determined A_f and x_f. Fig. 5 shows the calculated time dependence of x for one sample each of CdTe, CdSe and CdS. A, of course, continues to decrease with time in all cases. According to these calculations x reaches a constant value within the first several hours for CdS and CdSe, whereas it continues to decrease indefinitely for the tellurides. The results of the calculations may not be too accurate for CdS and CdSe, since their x values are so close to 0.5. In this region, the p–x relation is not exact enough to be used for a quantitative calculation because the accurate measurement of the p–T relation is very difficult near the stoichiometric composition. In addition the measured deviation of x from 0.5 is not much larger than the experimental error Δx. The calculated $A(t)$ and $x(t)$ curves, therefore, are only qualitatively valid for CdS and CdSe. On the other hand, the accuracies of both the calculated and experimental values should be good for the tellurides, because their x values pass through the inaccurate region (roughly $0.49 < x < 0.51$) within the first hour of growth. The fact that for three samples of ZnTe the calculated values of A_f and x_f, which were obtained by using the same value of (μ_N/μ_M), agree well with the experimental values suggests that for this compound the present analysis is valid not only qualitatively, but also quantitatively.

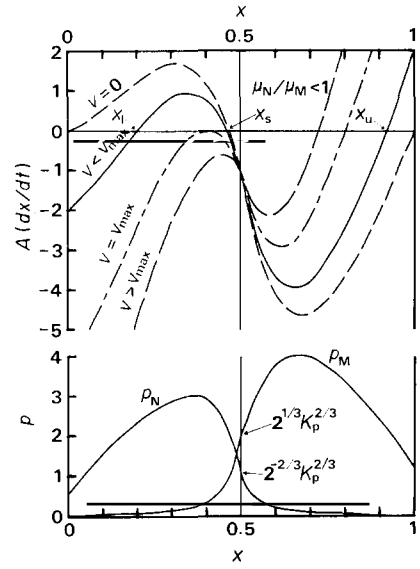

Fig. 6. Schematic curves of $A(dx/dt)$ and partial vapor pressures as functions of composition x for a II–VI compound.

6. General features of the variation in melt composition

In this section, we shall consider the general features of the variation in melt composition that follow from the rate equation (5b) and the characteristic p–x relations for II–VI compounds. These relations along the liquidus curve are shown schematically in the lower part of fig. 6. As x increases from 0.5, p_M initially increases because the activity of M atoms in the melt increases, but p_M reaches a maximum and then decreases because the saturated vapor pressure of the pure metal p_M^0 decreases as the temperature decreases along the liquidus curve. As x decreases from 0.5, a similar variation is obtained for p_N. For $0 < x < 0.5$, p_M increases monotonically with increasing x; for $0.5 < x < 1$, p_N decreases monotonically with increasing x. At all points along the liquidus curve, p_M and p_N are related through the equilibrium constant $K_p = p_M\sqrt{p_N}$.

The upper part of fig. 6 shows schematically the $A(dx/dt)$ versus x curves calculated by using eq. (5b) with various crystal growth rates and with (μ_N/μ_M) less than 1. (Since A is always positive, (dx/dt) and $A(dx/dt)$ always have the same sign.) The important features of these curves are as follows:

(1) For sufficiently low but non-zero growth rates, (dx/dt) crosses zero at three points denoted by x_1, x_s, and x_u. The central point x_s is the only one of the three at which $(d/dx)(dx/dt)$ is negative. If the starting composition x_i lies between x_1 and x_u, as it does in the growth experiments, the melt composition eventually reaches x_s and then remains constant.

(2) If $(dx/dt) > 0$ at $x = 0.5$, $x_s > 0.5$ (metal excess); if $(dx/dt) < 0$ at $x = 0.5$, $x_s < 0.5$ (chalcogen excess). Since $p_M = 2p_N$ at $x = 0.5$, according to eq. (5b) the sign of (dx/dt) at $x = 0.5$ is positive if $(\mu_N/\mu_M) > 1$ and negative if $(\mu_N/\mu_M) < 1$. Therefore $x_s > 0.5$ if $(\mu_N/\mu_M) > 1$, but $x_s < 0.5$ if $(\mu_N/\mu_M) < 1$; the latter case is shown in fig. 6. Thus the melt becomes enriched in the more slowly diffusing component.

(3) If the growth rate v exceeds a value designated as v_{max}, the third term in eq. (5b) becomes so large compared to the first two that there is no longer a stable point, and the melt composition moves indefinitely in one direction.

For the tellurides, the sum of the first two terms in eq. (5b) is less than the third term except at very low growth rates. Under the present experimental conditions, for example, v_{max} is estimated to be about 0.002 mole/h (1 mm/h) for ZnTe and 0.005 mole/h (2 mm/h) for CdTe. (The growth rate v of 0.0025 mole/h corresponds approximately to the growth velocity v' of 1 mm/h for the crucible used in the present study.) The calculated curves of $A(dx/dt)$ for CdTe are drawn in fig. 7. Since the growth velocity used for the tellurides is in the range from 3 to 10 mm/h, where no stable point can exist, the final melt composition deviates considerably from $x = 0.5$ and depends strongly on the growth conditions. In contrast with the telluride case, p_{Se} increases rapidly as x decreases below 0.5 in the Cd–Se system. Therefore, when $v' = 5-10$ mm/h, the second term in eq. (5b) is much larger than the

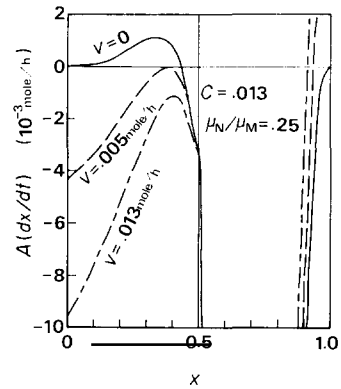

Fig. 7. Calculated curves of $A(dx/dt)$ as a function of composition x for CdTe.

third one. For the present conditions, v'_{max} for CdSe is estimated to be about 70 mm/h: at the growth velocities usually used, there exists a stable point x_s which is close to 0.5. CdS behaves similarly, with v'_{max} estimated to be about 2300 mm/h. Unfortunately, there are no experimental data for the p–x and the T–x relations of ZnS and ZnSe. However, their melting temperatures (1720 °C for ZnS and 1530 °C for ZnSe) are very high compared to those of ZnTe and CdSe. This means that the saturated vapor pressure of a pure element p^0 in Jordan's expression is very high around $x = 0.5$. In addition, the vapor pressures of ZnS and ZnSe are high at temperatures near the melting points (more than several atmospheres) even if x is very close to 0.5. For these compounds, therefore, at the usual growth rates the third term in eq. (5b) is expected to have only a slight effect on dx/dt, and the stable composition x_s is likely to be very close to 0.5 and will still exist even if v becomes quite large.

From table 2 and the general features of the melt composition described above, we obtain the experimentally determined order for the material parameter μ as

$$\mu_S, \mu_{Zn} > \mu_{Cd} > \mu_{Se} > \mu_{Te}.$$

We have neither experimental data nor accurate theoretical expressions for the values of μ in the present system. However μ would, in principle, be expressed as

$$\mu = \frac{1}{Sc}\left(\frac{1}{m} + \frac{1}{m_0}\right)^{1/2}, \tag{6}$$

where Sc is the effective collision cross section, and m and m_0 are respectively the masses of the component gas atoms or molecules and of the inert gas atoms. Among either the Group II_b elements or Group VI_b elements, μ should be increased by decreasing the atomic mass, which decreases the atomic or molecular diameter and therefore Sc. This is consistent with the experimental results. We need further investigations of μ or D itself to predict the relationship of μ for the Group II_b element to that for the Group VI_b element. However it should be mentioned that among all five elements the experimentally determined μ increases with decreasing mass of the component gas species, if we assume the species to be monatomic and diatomic for the Group II_b and the Group VI_b elements, respectively.

7. Conclusions

Two principal conclusions can be drawn concerning the melt composition during the crystal growth of II–VI compounds in a high-pressure furnace:

(1) The direction of the melt's deviation from the stoichiometric composition is fixed by the difference between the diffusion coefficients of the metal vapor atoms and chalcogen vapor molecules.

(2) If the partial pressure of the less rapidly diffusing component gas increases rapidly enough as the melt deviates from the stoichiometric composition, the melt composition has a stable point even at high crystal growth rates, as in the case of the sulfides and selenides. If not, there is no stable composition even at low growth rates, and the melt continues to deviate increasingly from the stoichiometric composition during growth, as in the case of the tellurides.

When the melt composition is not stoichiometric, the excess element must be rejected into the melt at the solid–liquid interface, making crystal growth more difficult. The large deviations observed in the melt compositions of the tellurides might be one of the factors which limit their growth rates to rather low values.

Acknowledgement

The authors wish to thank Mr. A. Yoshidome and Mr. H. Nishiura for their help with the electron microprobe analysis, and Mr. K. Shimada for helpful discussions on the wet chemical analysis.

Appendix: Derivation of equation (1)

In the present case, the diffusion equation

$$\frac{\partial n}{\partial t} = D\frac{\partial^2 n}{\partial y^2} \tag{A1}$$

can be solved under the following conditions,

$$\frac{\partial n}{\partial t} = 0, \tag{A2}$$

$$n = n_c \qquad \text{at } y = 0, \tag{A3}$$

$$n = 0 \qquad \text{at } y = d, \tag{A4}$$

where n is the number of atoms or molecules of the component vapor in unit volume, n_c is this number inside the crucible, y is the distance and d is the average thickness of the crucible wall or the average length of

the migration path. The condition (A2) is derived from steady-state diffusion, that is, from the assumption of the change rate of n in the crucible wall to be fast enough compared to the change rate of n_c. The condition (A4) results from the fact that the strong thermal convection current of the inert gas in the furnace rapidly removes the component gases as soon as they leave the crucible.

The solution of eq. (A1) is

$$n = n_c\,(1 - y/d), \tag{A5}$$

and the leakage rate of the component gas can be given as,

$$Y \propto D \left| \frac{dn}{dy} \right| \propto D n_c, \tag{A6}$$

namely, eq. (1) in section 5.

References

1) W. E. Medcalf and R. H. Fahrig, J. Electrochem. Soc. **105** (1958) 719.
2) A. G. Fischer, J. Electrochem. Soc. **117** (1970) 41C.
3) M. J. Kozielski, Phys. Status Solidi **31** (1969) K9.
4) A. S. Jordan, Met. Trans. **1** (1970) 239.
5) B. M. Kulwicki, Ph. D. Thesis, University of Michigan (1963).
6) L. R. Shiozawa, J. M. Jost and G. A. Sullivan, Final Technical Report, Contract AF33(615)2708, Aerospace Research Lab. USAF (1968).
7) M. R. Lorenz, J. Phys. Chem. Solids **23** (1962) 939.
8) A. S. Jordan and R. R. Zupp, J. Electrochem. Soc. **116** (1969) 1285.
9) A. Reisman, M. Berkenblit and M. Witzen, J. Phys. Chem. **66** (1962) 2210.
10) R. A. Burmeister, Jr. and D. S. Stevenson, J. Electrochem. Soc. **114** (1967) 394.
11) H. H. Woodbury, J. Phys. Chem. Solids **24** (1963) 881.
12) L. R. Shiozawa and J. M. Jost, Summary Report, ARL-69-0107, Contract F33615-68-C-1601, Aerospace Research Lab. USAF (1969) p. 46.